A New Analysis of Direct-Sequence Pseudonoise Code Acquisition on Rayleigh Fading Channels

Wern-Ho Sheen, *Member, IEEE,* and Huan-Chun Wang

***Abstract*—Accurate performance evaluation of direct-sequence pseudonoise code acquisition on Rayleigh fading channels is investigated in this paper. For fading channels the homogeneous Markov chain model, used to characterize the acquisition process over additive white Gaussian noise channels, is no longer valid due to the correlations between cell detections incurred by fading. Hence, the traditional direct and flow-graph approaches for performance evaluation of the code acquisition are not applicable to fading channels. In this paper, a new analysis is proposed for accurate evaluation of the acquisition performance on Rayleigh fading channels. The analysis is quite general and can include various search strategies, types of correlators, and test methods with different performance measures: probability mass function and/or moments of acquisition time. Analytical and simulation results show that the new method predicts the acquisition performance very accurately.**

***Index Terms*—Direct sequence spread spectrum, pseudonoise code acquisition, Rayleigh fading.**

I. Introduction

PSEUDONOISE (PN) code acquisition is one of the most challenging tasks in the design of a direct-sequence (DS) spread spectrum receiver. It has been a topic of intensive research for more than 20 years [1], [2]. PN code acquisition was investigated mainly for the traditional additive white Gaussian noise (AWGN) channels in the past [1]–[10]. The extension to time-variant multipath fading channels, however, has recently become more and more important because of the superiority of applying the DS spread spectrum technique to the personal and mobile communications, where the channel is modeled as a time-variant multipath fading one [11]–[15].

DS code acquisition methods may possibly be divided into different classes according to the types of searching strategies (serial, parallel, or hybrid), correlators (passive or active), test methods (fixed or variable dwell-time), and some others [1]–[10]. Generally speaking, the parallel search outperforms the serial search, the passive correlator outperforms the active correlator, and the variable dwell-time test outperforms the fixed dwell-time test, all at the expense of a larger system complexity and/or a more complicated performance analysis. Two approaches, namely direct and flow-graph approaches, have been applied extensively for analyzing the performance of an acquisition system, probability mass function (PMF), and/or moments of the acquisition time [3], [8]–[10]. Theoretically, these two methods are only applicable to the AWGN channels because the homogeneous Markov chain modeling of the acquisition process, a fundamental assumption of these methods, is no longer valid for time-variant multipath fading channels due to the channel memory incurred by fading; an analysis without considering the correlations due to fading may only be considered as an approximation. Unfortunately, as to be shown, the analysis error due to no consideration on the channel correlations can be very large, especially for the acquisition system based on passive correlators. A more accurate analysis for fading channels is yet to be found.

Very recently, attempts have been given to analyze code acquisition operating on time-variant multipath fading channels [13]–[15].[1] In these analyses, by assuming that the channel coherence time is smaller than the time between correct cells detections, the correlations incurred by fading between correct cells can be safely neglected. (Unfortunately, this approximation is only justifiable for the acquisition systems based on active correlators.) Hence, for this type of system, the homogeneous Markov chain model can still be considered as valid, and the direct and flow-graph approaches can be employed for performance evaluation as in the AWGN channels, except that the correlations incurred by fading within the correct cell detection need to be taken into account.

In this paper a novel accurate analysis, based on direct approach, is proposed for DS code acquisition operating over Rayleigh fading channels. Thanks to the direct approach, the analysis is general enough to include various search strategies, correlators, and test methods with different performance measures: PMF and/or moments of the acquisition time.

The remainder of this paper is organized as follows. The system model is described in Section II, where the acquisition system based on passive correlators is used as an example for analysis. Section III presents our new analytical method that can take into account the correlations incurred by fading. Section IV gives numerical results that illustrate the effects of fading correlations on the acquisition performance. Finally, the paper is concluded in Section V.

Manuscript received June 11, 1999; revised September 17, 2001.

W.-H. Sheen is with the Department of Communication Engineering, National Chiao Tung University, Hsinchu 300, Taiwan R.O.C. (e-mail: whsheen@em.nctu.edu.tw).

H.-C. Wang is with the Wireless Communication Department, Computer and Communication Laboratories, Industrial Technology Research Institute, Hsinchu 310, Taiwan R.O.C.

Publisher Item Identifier S 0733-8716(01)09087-4.

[1]The acquisition systems and channel models considered in [13] are more general than that in [14] and [15].

II. System Model

A. Channel Model

A popular channel model for the terrestrial personal and mobile communication environment is given by the impulse response

$$h(t;\,\tau) = \sum_{l=1}^{N} \alpha_l(t) e^{j\theta_l(t)} \delta(\tau - \tau_l) \tag{1}$$

where

N	path number;
τ_l	path delay;
$\alpha_l(t)$ and $\theta_l(t)$;	Rayleigh fading and uniform random phase over $[0,\,2\pi)$, respectively.

τ_l is assumed to be fixed during the time of code acquisition because the received signal will only experience a small code Doppler shift for the terrestrial personal and mobile communication environment. For the case of $N > 1$, the conditions for the true acquisition are more complicated to characterize for a code acquisition system. For example, assume that there are $\tilde{N} \leq N$ fingers in the RAKE receiver, then one may want to search the largest $\tilde{N}$ paths one after one; only after the $\tilde{N}$ largest paths have been found, the acquisition process would then be declared to be successful. In this paper, our main concern is how the correlations incurred by fading can be taken into account in the analysis. Hence, only the case of $N = 1$ will be considered for simplicity. The extension to the cases with $N > 1$ is straightforward because of the use of direct approach.

B. Acquisition Process

As in nearly all literature, the code phase uncertainty[2] of an acquisition system is divided into cells, with a cell size to within the lock-in range of the code tracking loop used for fine code alignment. The acquisition system then searches through the code phases and determines which cells are the correct cells, according to some type of code phase correlators, search strategies, and test methods. As usual, the correct cells will be denoted as the H_1 cells (hypothesis H_1) and the incorrect cells as the H_0 cells (hypothesis H_0), respectively. In practice, there may be more than one correct cell. For simplicity of presentation, however, only the case of one correct cell will be used as an example, although the method applies equally well to the more general case with more than one correct cell. Two types of decision errors may occur when detecting a cell, namely false dismissal of the H_1 cell and false alarm of the H_0 cells. When a false alarm occurs, the synchronization will be turned to code tracking for fine alignment. In this case, it is assumed that the false alarm can always be detected after some fixed or random time, and the synchronization will be turned back to the code acquisition. Hence, the search process for the correct cell will go on and on until the true acquisition is accomplished.

Thanks to the use of direct approach, the method is applicable to various search strategies, correlators, and test methods, as will be described. For simple presentation, however, only the serial search (straight line) system based on passive correlators will be used as an example for the analysis in the following.

C. Code Acquisition Based on Passive Correlators

Fig. 1 is a code acquisition system based on passive correlators. $r(t)$ is the received signal, given by

$$r(t) = \Re\left\{\sqrt{2P}\sum_k \alpha(t) c_k h(t - kT_c - \tau) e^{j(w_c t + \theta(t))}\right\} + n(t) \tag{2}$$

where

$\Re$	operation of taking the real part;
P	transmit power;
$\alpha(t)$ and $\theta(t)$	gain and phase of the fading channel, respectively;
c_k	PN sequence with period L;
$h(t)$	shaping function;
T_c	chip duration;
τ	code phase to be estimated;
w_c	carrier frequency;
$n(t)$	additive white Gaussian noise with one-side power spectral density of N_0 watts/Hz.

Define $x_c(t) = \alpha(t)\cos[\theta(t)]$ and $x_s(t) = \alpha(t)\sin[\theta(t)]$. Then, for Rayleigh fading $x_c(t)$ and $x_s(t)$ are independent and identical distributions (i.i.d) Gaussian processes.

The received signal, after I/Q down conversion, chip matching, and sampling, is digitally correlated with the local PN code. The correlators' outputs are then squared and summed to form the test variable t_k. If t_k is greater than a threshold, say V_{T_1}, then the acquisition will enter a verification mode or the synchronization will be turned to code tracking. Otherwise, the search for the H_1 cell continues. Assume perfect chip synchronous sampling, then the outputs of the correlators are given by

$$y_u(k) = \frac{1}{\sqrt{L\sigma_x^2}} \sum_{j=0}^{L-1} x_u(k+j) c_{k+j} c_j + \frac{1}{T_c\sqrt{LP\sigma_x^2}} \sum_{j=0}^{L-1} n_u(k+j) c_j \qquad u = c,\, s \tag{3}$$

where $x_u(k) \triangleq x_u(kT_c)$, $\sigma_x^2 = \mathrm{E}[x_u^2(k)]$, and $\{n_u(k)\}$ are i.i.d. zero-mean Gaussian variables with variance equal to $N_0/2 \cdot T_c$. In the terrestrial mobile and personal communications, the fading rate is much smaller than $1/(LT_c)$ (usually the symbol rate), and hence $x_u(t)$ can be considered to be fixed during the duration of LT_c. Note that in Fig. 1(b) we have assumed full period correlation, i.e., the number of correlation chips is equal to L. In practice, however, the number of correlation chips may be much smaller than L (partial period correlation) for a large L, and there will be code-self noise in the detection of H_0 cells. In this case, if the code-self noise is modeled as a Gaussian noise

[2]It is well known that in addition to increase the total cell numbers, frequency offset causes signal-to-noise ratio (SNR) degradation by the value

$$\left[\frac{\sin(\pi L \Delta f T_c)}{\sin(\pi \Delta f T_c)}\right]^2$$

where L is the correlation length, and Δf is the frequency offset. For simple presentation, we do not include this effect in the analysis, although it can be easily done so.

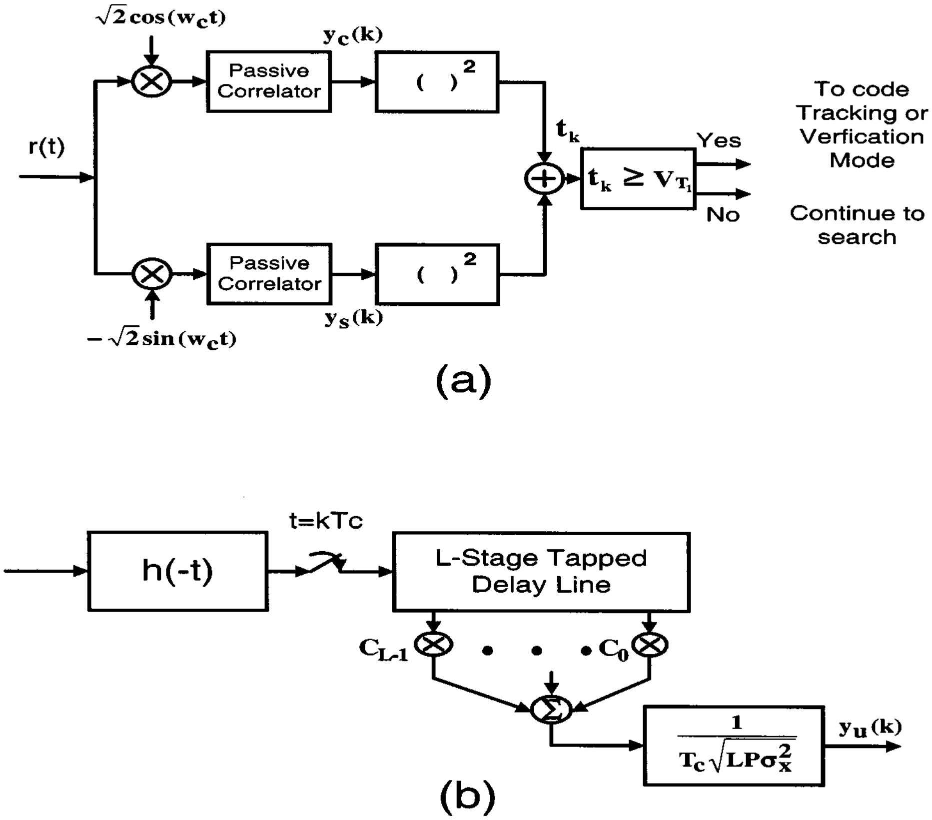

Fig. 1. (a) Code acquisition based on passive correlators. (b) Passive correlator.

as is usually done in the literature [16], our method of analysis described below applies as well.

Under H_0, by using the property that the out-of-phase correlation of a PN sequence can be approximated as zero for full period correlation, one has

$$y_u(k) = \frac{1}{T_c\sqrt{LP\sigma_x^2}} \sum_{j=0}^{L-1} n_u(k+j)c_j, \qquad u = c,\, s \tag{4}$$

which is a zero-mean Gaussian variable with variance equal to

$$\frac{N_0}{2PT_c\sigma_x^2} = \frac{1}{\gamma_c} \tag{5}$$

where

$$\gamma_c \triangleq \frac{2PT_c\sigma_x^2}{N_0} \tag{6}$$

is the received signal to noise density ratio. Define $\mathcal{R}_y(k-l) \triangleq \mathrm{E}[y_u(k)y_u(l)]$. It can be shown that the correlation coefficient of $y_u(k)$ and $y_u(l)$ is

$$\rho_y(k-l) \triangleq \frac{R_y(k-l)}{R_y(0)} = \begin{cases} 1/L \displaystyle\sum_{j=0}^{L-|k-l|-1} c_j c_{j+|k-l|}, & 0 < |k-l| \le L-1 \\ 0, & \text{o.w.} \end{cases} \tag{7}$$

For a large enough L, $\rho_y(k-l) \approx 0$, $k \neq l$. Hence

$$t_k \triangleq y_c^2(k) + y_s^2(k) \tag{8}$$

are well approximated as independent variables under H_0, as in the AWGN channels. This is not the case under H_1, however, due to the channel memory incurred by fading. In this case, we have

$$\rho_y(k-l) = \begin{cases} 1, & k = l \\ \dfrac{L\rho_x(k-l)}{L+1/\gamma_c}, & |k-l| = jL \end{cases} \tag{9}$$

where $\rho_x(k-l)$ is the correlation coefficient of $x_u(k)$ and $x_u(l)$, and j is a positive integer. This correlation between H_1 cells renders the homogeneous Markov chain model, a fundamental assumption of the direct and flow-graph approaches for the performance analysis on AWGN channels, invalid. A new method that can take this correlation into account needs to be devised for performance analysis. From (7), it is also easy to see that the detections between H_1 and H_0 cells are approximately independent.

III. New Analysis

In this section, the acquisition system with no verification mode will be used as an example to illustrate the new analytical method. Some performance examples with a verification mode are given in Section IV.

A. Signal Flow Diagram

As in [3], the acquisition process can be represented by a signal flow graph. For example, the signal flow graph for the straight-line search is shown in Fig. 2(a), where π_i is the probability that the ith cell is the starting cell, $H_0(z)$ is the gain characterizing the detection of an H_0 cell, and $H_{D|\underline{k}}(z)$ and $H_{M|\underline{k}}(z)$ are the gains for the correct detection and false dismissal of the H_1 cell, respectively, with $\underline{k}$ to denote the fact that the detection of the H_1 cell at present time depends on previous H_1 cells detections. Let k_j be the time of doing jth detection of the H_1 cell. Then, for the ith detection of the H_1 cell, $\underline{k} = (k_1, k_2, \ldots, k_i)$. That is, the ith detection of the H_1 cell at the time k_i depends on the H_1 cell detections at the times of $k_1, \ldots, k_{i-1}$. Recall that the detections of H_0 cells are independent of one another.

For an acquisition system with no verification mode

$$H_0(z) = P_f \cdot z^{1+K_p} + (1 - P_f) \cdot z \tag{10}$$

$$H_{D|\underline{k}}(z) = P_{D|\underline{k}} \cdot z \tag{11}$$

$$H_{M|\underline{k}} = P_{M|\underline{k}} \cdot z \tag{12}$$

where

P_f	probability of false alarm;
K_p (in T_c)	penalty time assumed to be constant;
$P_{D\|\underline{k}}$ and $P_{M\|\underline{k}}$	probabilities of the correct detection and false dismissal, respectively.

The unit time in (10)–(12) is T_c. Fig. 2(a) can be further simplified as in Fig. 2(b). At this point, one might attempt to apply Mason's formula to obtain the generating function $P_{T_a}(z)$ of the acquisition time T_a, as in the AWGN case. (In effect, $P_{T_a}(z)$ contains all the information about the PMF of the acquisition time T_a.) Unfortunately, Mason's formula does not apply in a fading channel case because $H_{D|\underline{k}}(z)$ and $H_{M|\underline{k}}$ are now functions of time. A new method is required for the performance evaluation.

B. Calculation of P_f, $P_{D|\underline{k}}$, and $P_{M|\underline{k}}$

From definition and (8), it is easy to see that under H_0, $\{t_k\}$ are i.i.d. central chi-square variables, and

$$\begin{aligned} P_f &\triangleq P_r\{t_k \geq V_{T_1} | H_0\} \\ &= \exp[-\gamma_c V_{T_1}]. \end{aligned} \tag{13}$$

On the other hand, however, the evaluation of $P_{D|\underline{k}}$ and $P_{M|\underline{k}}$ becomes much more involved due to the correlations incurred by fading. Since $P_{M|\underline{k}} = 1 - P_{D|\underline{k}}$, we will only consider $P_{D|\underline{k}}$. Assume that $P_{D|\underline{k}}$ for the ith detection of the H_1 cell is of interest. From the definition

$$P_{D|\underline{k}} \triangleq P_r\left\{t_{k_i} \geq V_{T_1}, t_{k_{i-1}} < V_{T_1}, \ldots, t_{k_1} < V_{T_1} | H_1\right\}. \tag{14}$$

Unlike the H_0 case, $\{t_{k_j}\}$ now are correlated central chi-square distributed variables, and, to our best of knowledge, there is still no easy way for the evaluation of (14). In the following, a novel method is proposed to evaluate $P_{D|\underline{k}}$ to the desired accuracy.

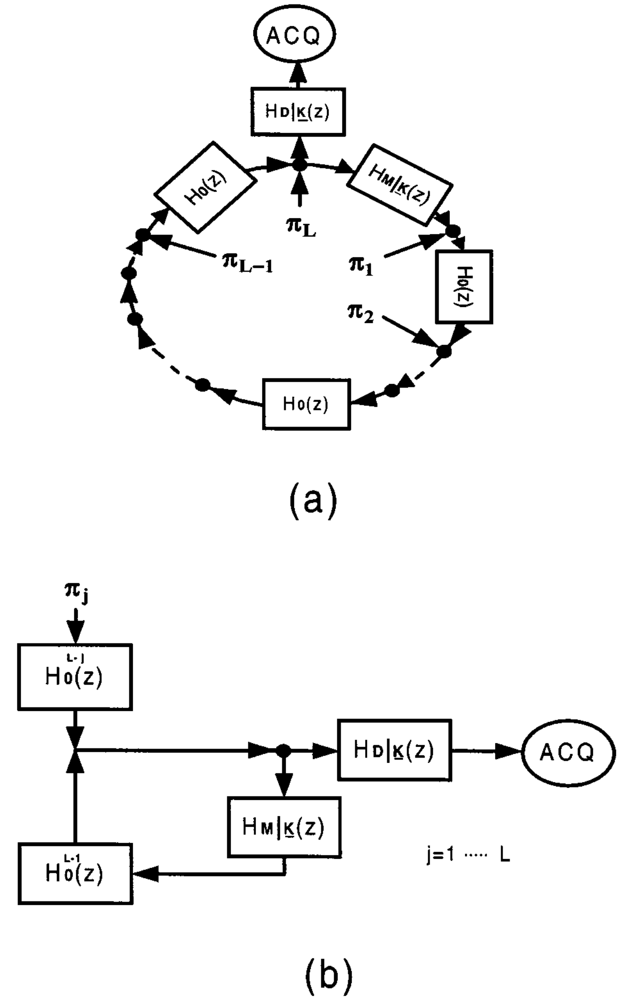

Fig. 2. (a) Signal flow diagram for the straight-line search. (b) Simplified signal flow diagram.

To begin with, the following definitions are necessary (also see [15]).

Definition 1 [17]: A symmetric random matrix $\mathcal{S}$ of dimension $\kappa \times \kappa$ is said to have a Wishart distribution $W_\kappa(n, \Sigma)$ with n degrees of freedom and parameter Σ, if $\mathcal{S}$ can be written as

$$\mathcal{S} = \sum_{l=1}^{n} \boldsymbol{\psi}_l^T \boldsymbol{\psi}_l \tag{15}$$

where $\boldsymbol{\psi}_l = (\psi_{1l} \cdots \psi_{\kappa l})$, $l = 1, \ldots, n$, are independently distributed normal κ-vectors with zero mean and covariance matrix Σ, where T denotes the operation of transpose. The matrix $\mathcal{S}$ is called the Wishart matrix.

Definition 2 [17]: Let $\mathcal{S}$ be the Wishart matrix with the distribution $W_\kappa(n, \Sigma)$. The joint distribution of the diagonal elements of $\mathcal{S}$ given by

$$s_{mm} = \sum_{l=1}^{n} \psi_{ml}^2, \qquad 1 \leq m \leq \kappa \tag{16}$$

is called the κ-variate central chi-square distribution with n degrees of freedom and parameter Σ, denoted by $\chi_\kappa^2(n, \Sigma)$. With these definitions, we have the following theorem [15], [18].

Theorem: If a $\kappa \times \kappa$ covariance matrix $\Sigma > 0$ (positive definite) can be factorized as

$$W\Sigma W - I_\kappa = BB^T \tag{17}$$

where $W = \mathrm{Diag}(w_1, \ldots, w_\kappa) > 0$, I_κ is the identity matrix with dimension $\kappa\times\kappa$, and $B = (\boldsymbol{b}_1^T, \ldots, \boldsymbol{b}_\kappa^T)^T$ is a $\kappa\times d$ matrix with rank d, then the PDF of the distribution $\chi^2_\kappa(n, \Sigma)$ is given by

$$f(s_{11}, \ldots, s_{\kappa\kappa}; n, \Sigma) = E\left(\prod_{j=1}^{\kappa} \frac{w_j^2}{2}\, g_{n/2}\left(\frac{w_j^2}{2}\, s_{jj},\, \frac{1}{2}\,\boldsymbol{b}_j\mathcal{S}\boldsymbol{b}_j^T\right)\right) \tag{18}$$

where the expectation is taken with respect to the $W_d(n, I_d)$-distributed Wishart matrix $\mathcal{S}$, and

$$g_r(x, y) = \begin{cases} \left(\dfrac{x}{y}\right)^{(r-1)/2} \exp[-(x+y)] I_{r-1}(2\sqrt{xy}), & x \geq 0 \\ 0, & \text{o.w.} \end{cases} \tag{19}$$

is the noncentral chi-square distribution with $2r$ degrees of freedom and the noncentrality parameter $y \geq 0$, where $I_r(x)$ the rth order modified Bessel function of the first kind. From Definition 2 and (8), it is easy to see that $\{t_{k_j}\}$, $j = 1, \ldots, i$ under H_1 is distributed as $\chi^2_i(2, \Sigma)$ with the covariance matrix Σ given by

$$\Sigma_{lm} = L\rho_x(l - m) + 1/\gamma_c \cdot \delta_{lm}, \qquad l, m \leq i \tag{20}$$

where

$$\delta_{lm} = \begin{cases} 1, & l = m \\ 0, & \text{o.w.} \end{cases} \tag{21}$$

Furthermore, let

$$W = \mathrm{Diag}\,(\sqrt{\gamma_c}, \sqrt{\gamma_c}, \ldots, \sqrt{\gamma_c}\,). \tag{22}$$

It follows that $W\Sigma W - I_i \geq 0$ (positive semidefinite) is real symmetric. Assuming that rank $[W\Sigma W - I_i] = d$, let $\lambda_1 \geq \lambda_2 \geq \cdots \geq \lambda_d$ be the positive eigenvalues of $W\Sigma W - I_i$,[3] then the matrix B in (17) can be obtained as

$$B = \Xi\Lambda^{1/2} \tag{23}$$

where $\Lambda = \mathrm{Diag}(\lambda_1, \ldots, \lambda_d)$ and $\Xi = (\boldsymbol{\xi}_1^T, \ldots, \boldsymbol{\xi}_d^T)$, and $\boldsymbol{\xi}_j^T$ is the $i \times 1$ orthonormal eigenvector associated with λ_j. Hence, by the described theorem, given $\mathcal{S} = S$, the random variables t_{k_j}, $j \leq i$ are independent with the conditional pdf

$$f_{t_{k_j}}(t_{k_j}\,|\,S, H_1) = \frac{\gamma_c}{2}\, g_1\left(\frac{\gamma_c}{2}\, t_{k_j},\, \frac{1}{2}\,\boldsymbol{b}_j S\boldsymbol{b}_j^T\right), \qquad j \leq i. \tag{24}$$

Recall that S has the Wishart distribution $W_d(2, I_d)$, $\boldsymbol{b}_j$ is the jth row of the matrix B, and [from (19)]

$$g_1(x, y) = \exp[-(x + y)] I_0(2\sqrt{xy}\,). \tag{25}$$

[3] In practice, the matrix $W\Sigma W - I_i$ can always be approximated as having a rank d, if $\lambda_j/\lambda_1 \approx 0$, $j > d$.

With (24), now (14) becomes

$$P_{D|\underline{k}} = \mathrm{E}\left[P_r\{t_{k_i} \geq V_{T_1} | H_1, \mathcal{S}\} \cdot \prod_{j=1}^{i-1} P_r\{t_{k_j} < V_{T_1} | H_1, \mathcal{S}\}\right]. \tag{26}$$

It is well known that

$$\int_{V_{T_1}}^{\infty} \frac{\gamma_c}{2}\left(\frac{\gamma_c}{2}\, t_{k_j}, \frac{1}{2}\,\boldsymbol{b}_j S\boldsymbol{b}_j^T\right) dt_{k_j} = Q_1\left(\sqrt{\boldsymbol{b}_j S\boldsymbol{b}_j^T}, \sqrt{\gamma_c V_{T_1}}\right) \tag{27}$$

where $Q_\cdot(\cdot, \cdot)$ is the Marcum generalized Q function. Hence

$$P_{D|\underline{k}} = \mathrm{E}\left[Q_1\left(\sqrt{\boldsymbol{b}_1 S\boldsymbol{b}_1^T},\, \sqrt{\gamma_c V_{T_1}}\right) \cdot \prod_{j=1}^{i-1}\left(1 - Q_1\left(\sqrt{\boldsymbol{b}_j S\boldsymbol{b}_j^T},\, \sqrt{\gamma_c V_{T_1}}\right)\right)\right]. \tag{28}$$

Many methods can be employed for the evaluation of the expectation in (28) [19]. The method based on the Monte Carlo integration will be used for the numerical examples in Section IV.

C. Direct Approach

In the direct approach [8], the search strategy is characterized by a functional, say $\varphi(i, m)$, where i denotes that the true acquisition is accomplished at the ith detection of the H_1 cell, and m is the starting cell. For example, using Fig. 2

$$\varphi(i, m) = (i - 1)(L - 1) + (L - m) \tag{29}$$

for the straight line search. Given $\varphi(i, m)$, then the generating function of the acquisition time T_a is given by

$$P_{T_a}(z) = \sum_{m=1}^{L} \pi_m \sum_{i=1}^{\infty} P_{T_a}(z|i, m) \tag{30}$$

where $P_{T_a}(z|i, m)$ is the generating function of T_a conditioned i and m. Define $\mathcal{E}_{(i,m)}$ to be the set of $\underline{k} = (k_1, k_2, \ldots, k_i)$ that lead to the true acquisition, conditioned on i and m. Then

$$P_{T_a}(z|i, m) = \mathrm{E}\left[\sum_{\underline{k}\in\mathcal{E}_{(i,m)}} B(z, \underline{k}) \cdot H_{D|k_i}(z|\mathcal{S}) \cdot \prod_{j=1}^{i-1} H_{M|k_j}(z|\mathcal{S})\right] \tag{31}$$

where $B(z, \underline{k})$ is the term in $H_0^{\varphi(i, m)}(z)$ associated with the time sequence $\underline{k}$. For the cases with different search strategies, i.e., more than one H_1 cell and/or more than one path, the only difference in the analysis is to use different functionals $\varphi(i, m)$; the method has a broad range of applicability in this aspect.

Two observations are important regarding the calculation of (30). First, the infinite sum must be approximated by just including $i = 1$ to $i_{\max}$. (In our numerical examples, the maximal $i_{\max} = 100$.) Second, given $i_{\max}$ the sets $\mathcal{E}_{(i,m)}$, $i = 1 \cdots i_{\max}$, $m = 1 \cdots L$ can be enumerated first, and then B

and $\mathcal{S}$ can be generated for all $\underline{k}$s of interest in (30). As a result, the expectation operation only needs to be performed once in the evaluation of $P_{T_a}(z)$ that reduces the complexity of this method very significantly. That is, we have

$$P_{T_a}(z) \approx \mathrm{E}\left[\sum_{m=1}^{L} \pi_m \sum_{i=1}^{i_{\max,}} \sum_{\underline{k}\in\mathcal{E}_{(i,\,m)}} B(z,\, \underline{k}) H_{D|k_i}(z|\mathcal{S}) \cdot \prod_{j=1}^{i-1} H_{M|k_j}(z|\mathcal{S})\right]. \quad (32)$$

Of course, for each term in (32) only the $\boldsymbol{b}_k$ with those $k \in \underline{k}$ are needed in the evaluation of the associated $H_{D|k_i}(z|\mathcal{S})$ and $H_{M|k_j}(z|\mathcal{S})$ $j = 1, \ldots, i-1$.

IV. Numerical Examples

The Jakes' two-dimensional (2-D) isotropic scattering channel model and simulation method [20] are adopted in the following numerical examples. In the model, the correlation function of the in-phase and quadrature-phase fading components is given by

$$\mathrm{E}[x_u(t+\tau)x_u(t)] = \sigma_x^2 J_0(2\pi f_D \tau), \qquad u = c,\, s \quad (33)$$

where f_D is the maximum Doppler shift, and $J_0(x)$ is the zeroth-order Bessel function of the first kind. Three fading rates, namely $f_D/R_b = 0.0$, $f_D/R_b = 0.01$, and $f_D/R_b = 0.001$ are considered, where $R_b = 1/(LT_c)$. As mentioned, the Monte Carlo integration is used to evaluate the expectation over the Wishart distribution $W_d(2,\, I_d)$ required in (28), although the other integration algorithms [19] may also be used. It has been found that $d \le 5$ for all the numerical results. Also, less than 10^4 samples are needed for the Monte Carlo integration to obtain the desired accuracy. For simplicity, only the worst case, that is $\pi_1 = 1$ and $\pi_j = 0$, $j = 2 \cdots L$, is used to illustrate the acquisition performance. $i_{\max} = 100$ and $T_p = 12L$ in all results. In practice, an active correlator with threshold crossing is usually employed as a lock detector during tracking. It is common that the correlation time is taken to be around ten times of that used in the code acquisition to ensure the detection of in-lock or out-of-lock conditions. In our examples, the correlation time (penalty time) of the lock detector is assumed to be 12 times that used in code acquisition.

Figs. 3–5 are the results for the acquisition system with no verification mode. Fig. 3 shows an example PMF of the acquisition time under different fading rates. ($V_{T_1} = 40.0$, normalized to $LP\sigma_x^2 T_c^2$). Also shown is the PMF (approximation) obtained with the traditional direct approach without considering the correlations incurred by fading. As is evident, the discrepancy between the true and approximate PMF is very large. In Fig. 3, the largest peak is located at $T_{acq} = 63$, which means that the event with $i = 1$ and no false alarm has the largest probability. The second peak is located at $T_{acq} = 63 + 12 \cdot 63$, which is associated with the event that $i = 1$ and one false alarm. Note that there is a total of 62 of this type of event.

Fig. 4 shows the performance of mean acquisition time as a function of the threshold V_{T_1} under various fading rates. Clearly, the traditional analysis may underestimate the mean acquisition time by a large margin depending on thresholds and fading rates. As expected, the analysis error is larger for a smaller fading rate because a smaller f_D means that the correlation due to fading will extend longer. Note that the mean acquisition time obtained with the traditional analysis is independent of fading rate. Also shown in the figure is the simulation mean acquisition time. As seen, the analytical and simulation results agree very well for all the range of thresholds. Simulations are done with 10^7 samples to obtain the desired accuracy. In Fig. 3 we do not have simulation results because it is too time-consuming to be really conducted.

Fig. 5 shows the minimum mean acquisition time (those obtained with optimum thresholds) versus γ_c under various fading rates. The optimum thresholds are obtained from Fig. 4, and, as seen, they depend on Doppler rate, SNRs, penalty time, and some other parameters. More than an order of analysis errors are observed with the traditional analysis, depending on the fading

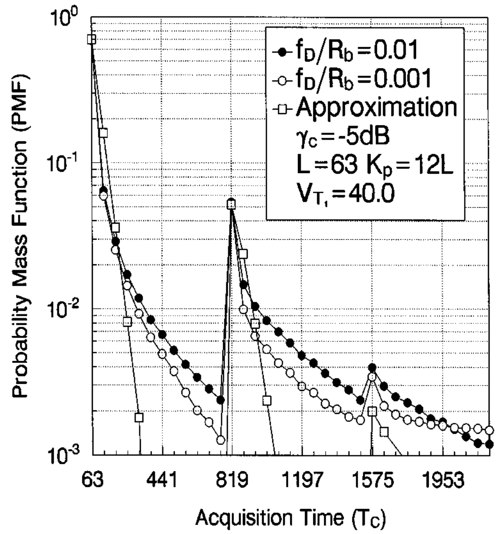

Fig. 3. Probability mass function of acquisition time with no verification mode.

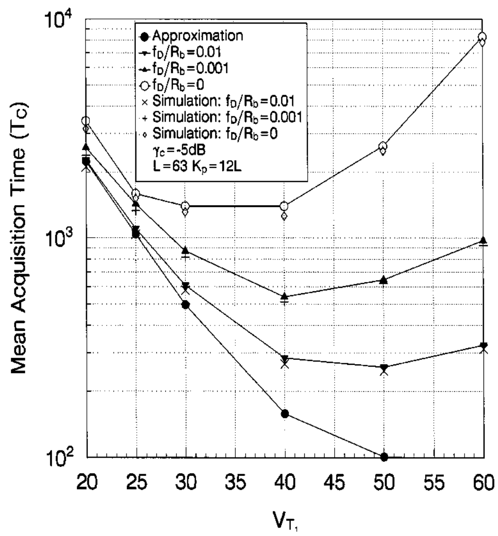

Fig. 4. Mean acquisition time versus threshold under different fading rates (no verification mode).

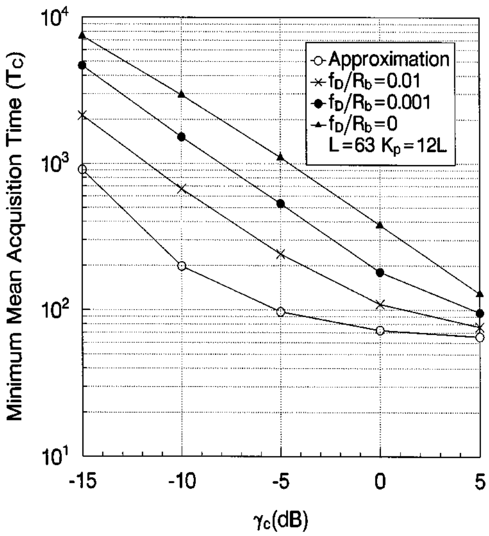

Fig. 5. Minimum mean acquisition time versus the received chip energy to noise ratio under different fading rates (no verification mode).

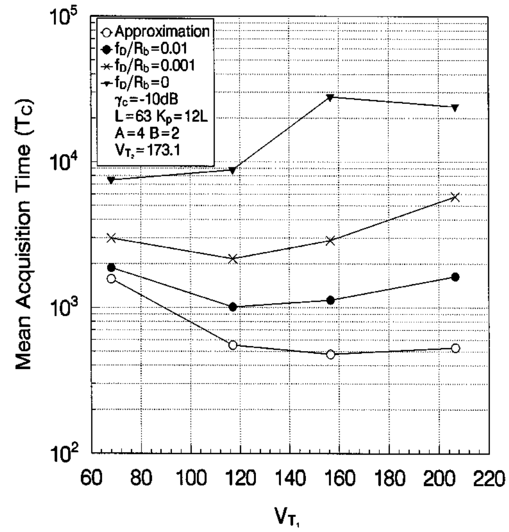

Fig. 7. Mean acquisition time versus the first threshold V_{T_1} under different fading rates (coincidence detector).

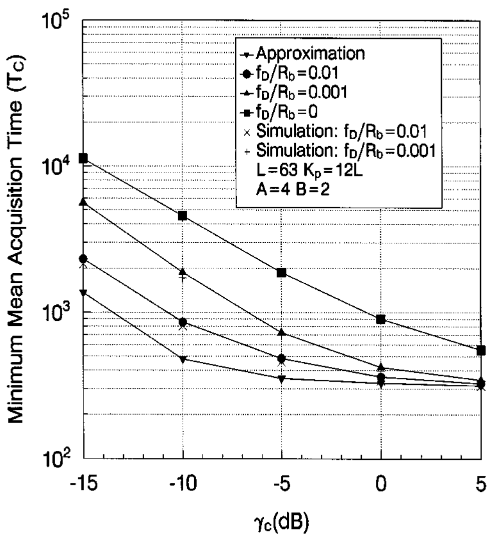

Fig. 6. Minimum mean acquisition time versus the received chip energy to noise ratio under different fading rates (coincidence detector).

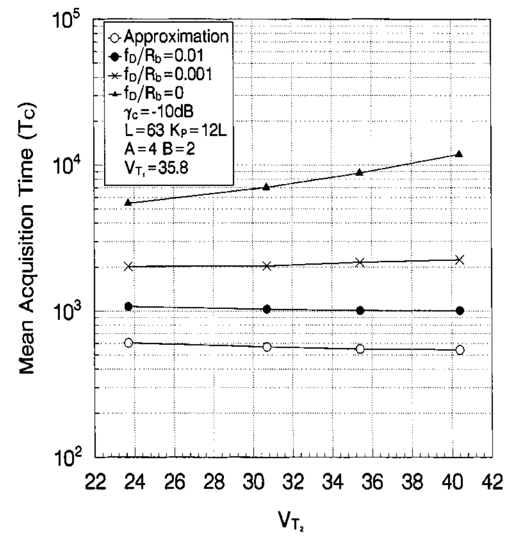

Fig. 8. Mean acquisition time versus the second threshold V_{T_2} under different fading rates (coincidence detector).

rates and SNRs. In addition, a smaller minimum mean acquisition time is obtained with a fast fading.

Figs. 6–8 are the results for the acquisition systems with a verification mode. The coincidence detector proposed in [3] is employed here. That is, after the first threshold V_{T_1} is exceeded, then an active correlator is activated and the test variable is compared to the second threshold V_{T_2}. If V_{T_2} is exceeded for B out of A times, a successful code acquisition will be declared. Otherwise, the search for the H_1 cell continues. The detailed analysis with a verification mode can be found in [15].

Fig. 6 shows the minimum mean acquisition time versus γ_c under various fading rates. Again, the traditional analysis may underestimate the true value by a large margin, depending on the fading rates and SNRs. Also, the analytical and simulation results agree very well in the figure. Figs. 7 and 8 are example mean acquisition times as a function of V_{T_1} (V_{T_2}) with V_{T_2} (V_{T_1}) being fixed, respectively. Similar results are observed in these two figures.

Finally, we note that the calculation of $P_{T_a}(z)$ in (32) is not as complicated as it appears to be. For example, it takes only few minutes to complete a point in Figs. 4–8 (in a commercially available work station with 10^4 samples for Monte Carlo integrations) instead of about one day by using simulation with 10^7 samples; the analytical method has a tremendous advantage in computation time over simulations. In addition, it is very difficult to use simulations to obtain accurate PMF of the acquisition time as the one shown in Fig. 3, especially to simulate with enough accuracy the rare events with probabilities smaller than 10^{-3}.

V. Conclusion

In this paper, a novel analytical method is proposed to analyze direct-sequence pseudonoise code acquisition systems over Rayleigh fading channels. The method is unique in that the channel memory incurred by fading between different cell detections can be taken into account. Thanks to the use of a direct approach, the method is quite general and can include various search strategies, correlators, and test methods with different performance measures: probability mass function and/or moments of acquisition time. Numerical results show that the new method predicts the acquisition performance very accurately, and the traditional analysis may suffer from a large analysis error, especially for the acquisition systems based on passive correlators.

REFERENCES

[1] M. K. Simon, J. K. Omura, R. A. Scholtz, and B. K. Levitt, *Spread Spectrum Communications*, MD: Computer Science Press, 1985, vol. III.

[2] R. L. Peterson, R. E. Ziemer, and D. E. Borth, *Introduction to Spread Spectrum Communications*. Englewood Cliffs, NJ: Prentice-Hall, 1995.

[3] A. Polydoros and C. L. Weber, "A unified approach to serial search spread-spectrum code acquisition—Part I: General theory," *IEEE Trans. Commun.*, vol. COM-32, pp. 542–549, May 1984.

[4] ——, "A unified approach to serial search spread-spectrum code acquisition—Part II: A matched filter receiver," *IEEE Trans. Commun.*, vol. COM-32, pp. 550–560, May 1984.

[5] Y. T. Su, "Rapid code acquisition algorithms employing PN matched filters," *IEEE Trans. Commun.*, vol. COM-36, pp. 724–733, June 1988.

[6] U. Cheng, "Performance of a class of parallel spread spectrum code acquisition schemes in the presence of data modulation," *IEEE Trans. Commun.*, vol. COM-36, pp. 596–604, May 1988.

[7] V. M. Jovanovic and E. S. Sousa, "Analysis of noncoherent correlation in DS/BPSK spread spectrum acquisition," *IEEE Trans. Commun.*, vol. 43, pp. 565–573, Feb./Mar./Apr. 1995.

[8] H. Meyr and G. Poltzer, "Performance analysis for general PN spread spectrum acquisition techniques," *IEEE Trans. Commun.*, vol. COM-31, pp. 1317–1319, Dec. 1983.

[9] V. M. Jovanovic, "Analysis of strategies for serial-search spread spectrum code acquisition-direct approach," *IEEE Trans. Commun.*, vol. COM-36, pp. 1208–1220, Nov. 1988.

[10] G. E. Corazza, "On the MAX/TC criterion for code acquisition and its application to DS-SSMA systems," *IEEE Trans. Commun.*, vol. 44, pp. 1173–1182, Sept. 1996.

[11] E. Sourour and S. C. Gupta, "Direct-sequence spread-spectrum parallel acquisition in a fading mobile channel," *IEEE Trans. Commun.*, vol. 38, pp. 992–998, July 1990.

[12] S. Tantaratana, A. W. Lam, and P. J. Vincent, "Noncoherent sequential acquisition of PN sequences for DS/SS communication with/without channel fading," *IEEE Trans. Commun.*, vol. 43, pp. 1738–1746, Feb./Mar./Apr. 1995.

[13] G. E. Corazza and A. Polydoros, "Code acquisition in CDMA cellular mobile networks—Part I: Theory," in *Proc. IEEE ISSSTA'98*, Sun City, South Africa, Sept. 2–4, 1998, pp. 454–458.

[14] W-H. Sheen and S. Chiou, "Performance of multiple-dwell pseudo-noise code acquisition with I/Q detector on frequency nonselective multipath fading channels," *Wireless Network*, vol. 5, pp. 11–21, 1999.

[15] H-C. Wang and W-H. Sheen, "Variable dwell-time code acquisition for direct sequence spread spectrum systems on time-variant Rayleigh fading channels," *IEEE Trans. Commun.*, vol. 48, pp. 1037–1046, June 2000.

[16] W. Zhuang, "Composite GPS receiver modeling, simulation and applications," Ph.D. dissertation, Univ. New Brunswick, Canada, 1992.

[17] N. C. Giri, *Multivariate Statistical Analysis*. New York: Dekker, 1996.

[18] T. Royen, "On some central and noncentral multivariate chi-square distributions," *Statistica Sininca*, vol. 5, pp. 373–397, 1995.

[19] A. R. Krommer and C. W. Ueberhuber, *Numerical Integration*. New York: Springer-Verlag, 1994.

[20] W. C. Jakes, Jr., *Microwave Mobile Communications*. New York: Wiley, 1974.

[21] H-C. Wang, "Pseudo-noise code acquisition for direct sequence spread spectrum systems on multipath fading channels," Ph.D. dissertation, National Chung Cheng Univ., Taiwan, July 1999.

Wern-Ho Sheen (S'89–M'91) received the B.S. degree from the National Taiwan University of Science and Technology, Taiwan, R.O.C., in 1982, the M.S. degree from the National Chiao Tung University, Taiwan, R.O.C, in 1984, and the Ph.D. degree from the Georgia Institute of Technology, Atlanta, in 1991.

From 1984 to 1993, he was with Telecommunication Laboratories, Taiwan, R.O.C, and from 1993 to 2001 he was with the Department of Electrical Engineering, National Chung Cheng University, Taiwan, R.O.C. Since 2001, he has been with the Department of Communication Engineering, National Chiao Tung University, Taiwan, R.O.C., where he is currently a Professor. His research interests include adaptive signal processing, spread spectrum communications, and personal and mobile radio systems.

Huan-Chun Wang was born in Hvalien, Taiwan, R.O.C., on January 14, 1969. He received the B.S.E.E degree from the Chung Yuan Christian University, Taiwan, R.O.C., in 1992, and the M.S.E.E. and Ph.D. degrees from the National Chung Cheng University, Chia-Yi, Taiwan, R.O.C., in 1994 and 1999, respectively.

Since October 1999, he has been with Computer and Communications Laboratories, Industrial Technology Research Institute, where he is mainly involved in the projects of wireless communications. His current research interests include communication theory, spread-spectrum communications, software defined radio, and personal and mobile communications.